

## Thermal and quantum nucleation of $^4\text{He}$ crystals in aerogel

H. Matsuda, A. Ochi, R. Isozaki, R. Masumoto, R. Nomura, and Y. Okuda

*Department of Physics, Tokyo Institute of Technology, 2-12-1 O-okayama, Meguro, Tokyo 152-8551, Japan*

(Received 1 February 2013; published 15 March 2013)

Nucleation of  $^4\text{He}$  crystals from the metastable superfluid in high porosity silica aerogel was investigated by an optical measurement. Critical overpressures at which the first  $^4\text{He}$  crystal appeared during pressurization were measured 50 times at each temperature. Contrary to the intuitive pore-size-limited nucleation suggested in previous studies in small pores, the critical overpressure did show a characteristic temperature dependence, indicating that the critical size of nucleation is also temperature dependent. It is confirmed that quantum nucleation at low temperatures and thermal nucleation at high temperatures occur as in the case of bulk crystal. Nucleation in this high porosity material shows characters of nucleation in both bulk and pores.

DOI: [10.1103/PhysRevE.87.030401](https://doi.org/10.1103/PhysRevE.87.030401)

PACS number(s): 64.60.Q-, 64.70.D-, 67.25.D-, 67.80.bf

Crystallization of fluid confined in a small space is an ordinary natural phenomenon such as the freezing of water in soil [1]. But details of the physical process of that crystallization remain unclear due to the complicated processes in natural materials. Crystallization of superfluid  $^4\text{He}$  in a porous material is expected to be free from such complications as the viscous mass flows and the heat flows in pores. It is therefore suitable for use in unveiling the nature of crystallization in porous media. Furthermore, novel quantum phenomena are expected to take place in  $^4\text{He}$  at very low temperatures. In classical materials, nucleation of a stable phase occurs via the thermal activation at high temperatures. In condensed phases of He, the thermal activation ceases and a quantum tunneling plays a role in the nucleation at low enough temperatures [2–15].

Nucleation of a  $^4\text{He}$  crystal in bulk superfluid usually takes place at a small overpressure, 10 mbars at most, on a wall. It is a heterogeneous nucleation, which is closely related to the depinning of a  $^4\text{He}$  crystal pinned at that site on the wall [4–11]. Crystallization of  $^4\text{He}$  in porous materials is elevated to a much higher pressure than that in the bulk [16–22]. The crystallization has been believed to be initiated when the critical size of the nucleus becomes equal to the pore size with enough overpressure [16–18]. This crystallization process in pores is sometimes regarded as homogeneous nucleation because the depinning process would play a minor role in this activity at such high overpressure. However, it is not clear at all whether it is actually comparable to the homogeneous nucleation in bulk in all aspects. To distinguish it from the homogeneous nucleation in the bulk, we refer to it as pore-size-limited (PSL) nucleation in this Rapid Communication. It sounds a little strange that the heterogeneous nucleation is excluded in porous materials which should have stronger disorder than the bulk. Since crystals do not wet the pore surface, a crystal with large curvature comparable to the pore size can never be stabilized at small overpressure; this is the reason PSL-nucleation occurs at much higher overpressures. Though the nucleation process is assumed in porous materials, details of the nucleation are lacking due to the difficulty in studying the dynamics by the blocked capillary method. Neither the quantum and thermal nucleation nor the metastability of superfluids have been clearly identified in porous materials.

Once the critical size is determined by the pore size, the corresponding critical overpressure is automatically fixed, and thus the PSL-nucleation model implies a temperature independent shift of the crystallization pressure. This is the case of nucleation in small pore materials [16–19]. If the pore size is comparable to or even larger than the critical size of the homogeneous nucleation, we as yet have no idea of what happens in the temperature dependence of the critical pressures. It is of particular interest to investigate the crystallization in highly porous materials with large pore sizes and to identify a possible precursor to the homogeneous nucleation which could be either thermal or quantum. We used a variable-volume cell which allowed us to investigate the nucleation process at various temperatures [21,22] and obtained an indication of crossover between thermal and quantum nucleation of  $^4\text{He}$  crystals in a high porosity aerogel.

Crystallization of  $^4\text{He}$  in aerogel exhibited a dynamical transition in the growth mode due to competition between thermal fluctuation and disorder. Crystal grows via creep at high temperatures and via avalanche at low temperatures [21,22]. The crystallization rate measurement has shown that the former is via thermal activation and the latter is via macroscopic quantum tunneling [22]. Another purpose of this study was to elucidate the origin of the dynamical transition from a different point of view.

The sample cell consisted of two chambers, a high-pressure (A) and a low-pressure (B) chamber, as shown schematically in Fig. 1(a). A part of both chambers was made of phosphor-bronze bellows which were connected by a copper rod. The volume of chamber A is controllable by the liquid in chamber B utilizing the larger cross section of the bellows of chamber B. The pressure of chamber A was measured by a capacitive pressure gauge (C) whose diaphragm was made of BeCu on the side wall of the chamber. The pressure in chamber B was measured by a pressure transducer installed in the room temperature gas handling system. Chamber B was pressurized at a fixed rate adjusted by a mass flow controller (Brooks model 5850E). Chamber A had two circular optical windows facing each other (not shown in Fig. 1 for clarity) and the interior detail is observable from room temperature. We illuminated chamber A through the back window by a parallel light beam (xenon lamp, USHIO UXL-151DO) and recorded the images

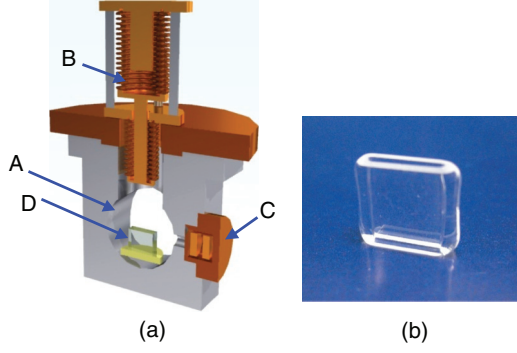


FIG. 1. (Color online) (a) Schematic view of the variable-volume cell. High-pressure (A) and low-pressure (B) chambers are connected by a rigid copper rod. The pressure of the bulk crystals was measured by a diaphragm-type pressure gauge (C). Aerogel (D) in a glass tube was placed in chamber A, which is visible through circular windows, which are not shown for clarity. (b) A flat glass tube to be filled with aerogel.

through the front window by a high-quality CCD camera (KEYENCE VW-100C).

Silica aerogel is a porous material consisting of nanometer scale silica particles with a highly open structure [23,24]. It has no clear pore size due to the fractal structure of silica particles. The mean distance between the silica strands is roughly 30 nm. We used a 98% porosity silica aerogel which was grown *in situ* in the thin and flat glass tube shown in Fig. 1(b). The inner space of the tube was 10 mm in height, 8 mm in width, and 1 mm in depth, and no gap existed between the aerogel and the inner wall of the tube. The bottom of the tube was glued to a glass plate and only the upper surface was open. Aerogel (D) was installed in chamber A.

The experimental procedure was as follows. The initial condensation of  $^4\text{He}$  was completed in chamber A in the supercritical region in order not to create a liquid-gas interface, which is known to damage the aerogel [25,26]. Chamber A was pressurized to the bulk crystallization pressure, and bulk crystals and superfluid liquid coexisted within it. At this stage, only the superfluid occupied the aerogel without an overpressure from the bulk crystallization pressure,  $\delta P = 0$ . We continued to pressurize chamber B at a fixed rate and at a constant temperature, and chamber A shrank. The bulk crystals outside the aerogel grew in chamber A and eventually completely occupied the outside; thereafter, the pressure in this chamber began to deviate from the bulk melting pressure,  $\delta P > 0$ . The liquid pressure in the aerogel also increased due to the stress-induced melting of the bulk crystals;  $^4\text{He}$  atoms entered the aerogel in the superfluid state as concluded in Ref. [22]. The appearance of the first crystal in the aerogel was visually observed both in the creep and avalanche regions and we recorded the critical overpressure  $\delta P_c$  in chamber A at which the first crystal was observed. The nucleation point in the aerogel was always the same: near the bottom [27]. This means that the aerogel was not perfectly uniform. After the crystals filled the aerogel, we depressurized chamber B until the crystals in the aerogel were completely melted. The melting began at approximately half of  $\delta P_c$  during the depressurization. True equilibrium crystallization pressure should exist between the two but is inaccessible in the inherently hysteretic system.

The next pressurization was then undertaken in the same way. This sequence was continued up to 50 times at a constant temperature and  $\delta P_c$  differed in each pressure sweep, as shown in Fig. 2 of Ref. [27]; the clear metastability of the superfluid liquid and the decay to the stable crystal phase were observed in the aerogel.

Cumulative distribution of  $\delta P_c$  was obtained at various temperatures to characterize the nucleation. We present  $\Sigma = \frac{N_0 - N}{N_0}$  as a function of overpressure;  $N$  is the number of nucleation events whose  $\delta P_c$  is less than  $\delta P$ , and  $N_0 = 50$  is the total number of pressure sweeps.  $\Sigma(\delta P)$  at two temperatures, 200 mK and 1.0 K, are shown as typical examples. As can be seen, distribution of the critical overpressure is temperature dependent.

Let us define  $\omega$  as the nucleation rate of the stable crystal in the metastable superfluid liquid; thus  $N$  decreases as time  $t$  proceeds, following the relation

$$N = N_0 \exp(-\omega t). \quad (1)$$

Thermal and quantum nucleation rates can be written as

$$\omega_t = \Gamma_t \exp\left(-\frac{E(\delta P)}{k_B T}\right) \quad (2)$$

and

$$\omega_q = \Gamma_q \exp\left(-\frac{2S_0(\delta P)}{\hbar}\right), \quad (3)$$

respectively [4,28,29]. Here,  $\Gamma$ 's are attempt frequencies and  $E$  and  $S_0$  are the energy barrier and the action for the nucleation, respectively. The thermal nucleation rate should increase with warming, while the quantum nucleation rate is temperature independent.

Assuming the fixed pressure sweep rate  $\delta P = ct$ ,  $\Sigma$  can be written by the nucleation rate as

$$\Sigma = 1 - \exp(-\omega t) = 1 - \exp\left(-\omega \frac{\delta P}{c}\right), \quad (4)$$

as shown in Ref. [4]. Since  $\Sigma$  is a steeply increasing function of  $\delta P$ , it is a good approximation in the case of thermal nucleation, as shown in Ref. [30], to expand  $E$  around the point  $\Sigma = 1/2$  as

$$\Sigma = 1 - \exp\left\{-\ln 2 \exp\left[\xi \left(\frac{\delta P}{\delta P_{1/2}} - 1\right)\right]\right\}, \quad (5)$$

where

$$\xi = -\frac{\delta P_{1/2}}{k_B T} \left(\frac{\partial E}{\partial P}\right)_{\Sigma=1/2}. \quad (6)$$

A similar relation holds for the quantum nucleation. We fitted  $\Sigma$  to Eq. (5) at various temperatures using two parameters,  $\delta P_{1/2}$  and  $\xi$ , which express the mean value of the critical overpressure and steepness of  $\Sigma$ , respectively. The lines in Fig. 2 are the fitted curves by this function.

We plot  $\delta P_{1/2}$  in Fig. 3 as a function of temperature to see the features of the nucleation.  $\delta P_{1/2}$  is nearly temperature independent below about 600 mK, decreases with warming, and turns around to increase above 1.0 K. This temperature dependence contradicts the constant shift of the crystallization pressure in aerogel to a higher pressure from the bulk which the PSL-nucleation model assumes; the critical size is not

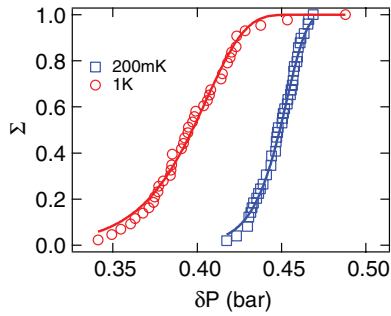


FIG. 2. (Color online) Cumulative distribution of overpressure below which the nucleation events occurred. Data at two temperatures 200 mK and 1.0 K are shown as typical examples. Lines are the fitting by Eq. (5). See text.

constant but is temperature dependent. Critical radius  $R_c$  can be estimated from the typical experimental value of  $\delta P_{1/2} \approx 0.45$  bars using the bulk value of  $\alpha$  as  $R_c = \frac{V_s}{V_l - V_s} \frac{2\alpha}{\delta P_{1/2}} \simeq 100$  nm; this value is a few times larger than the mean distance of the strands, about 30 nm [24].

Temperature independent critical overpressure is the expected feature of the quantum nucleation at low temperatures and its decrease with warming is that of thermal nucleation at high temperatures [4]. The obtained  $\delta P_{1/2}$  shows the crossover from the quantum to thermal nucleation of the  $^4\text{He}$  crystal in aerogel with warming. The increase above 1.0 K is not a typical behavior of the thermal nucleation. In this temperature range the crystallization pressure has a larger slope and the release of the latent heat becomes larger; it may be that the effect of the latent heat suppresses the thermal nucleation probability.

The dynamical transition temperature is about 625 mK for this aerogel; crystals grow via avalanche below 600 mK, via creep above 650 mK, and the two modes coexist between the two temperatures, as indicated by the dashed lines in Fig. 3.  $\delta P_{1/2}$  is temperature independent in the avalanche growth region and decreases with warming above the transition in the creep region. This fact indicates that quantum nucleation occurs in the avalanche growth region and thermal nucleation in the creep growth region. Although the critical overpressure is directly related to the initial appearance of the crystal from the metastable superfluid, it also suggests that all the crystal growth is quantum in avalanche and thermal in creep. The crystallization rate of  $^4\text{He}$  in aerogel was measured in

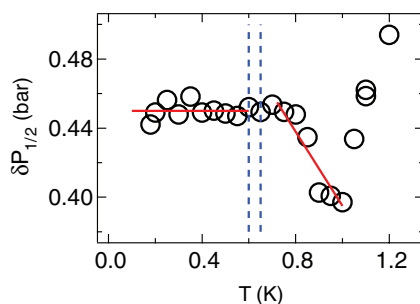


FIG. 3. (Color online) Mean critical overpressure as a function of temperature obtained from  $\Sigma(\delta P)$ . The two dashed lines indicate the transition region below (above) which crystals grow via avalanche (creep). Solid lines are a guide for the eyes. See text.

Ref. [22] and it was concluded that the avalanche growth is via quantum nucleation of crystals and the creep growth is via thermally activated interface motions. Thus, these two experiments on independent physical quantities, critical overpressure and crystallization rate in aerogel, consistently clarify the mechanism of the crystal growth modes.

The crystallization rate in Ref. [22] was temperature independent only in the low temperature limit and slightly suppressed with warming in the avalanche region. This suppression was attributed to the suppression of the quantum nucleation rate due to the dissipation. As found in this study, however, the critical overpressure, which is more directly related to the quantum nucleation rate, is temperature independent in the avalanche region and shows no sign of suppression due to dissipation. Crystallization rates via avalanche depend not only on the nucleation rate but also on the distribution of the final size of the nucleated crystals. The distribution does have the temperature dependence as shown in Ref. [22], and thus the suppression of the crystallization rate in Ref. [22] should be interpreted from the temperature dependence of the final size of the nucleated crystals.

What is the reason  $\delta P_{1/2}$  or the critical size is temperature dependent in aerogel? In low porosity materials such as Vycor glass, the pore radius is a few nm. If it is smaller than the critical size of homogeneous nucleation in the bulk state, nucleation size is fixed by the pore size and becomes temperature independent. In aerogel, the strand radius is a few nm, and the mean strand distance is rather large, about 30 nm [24]. It has no well-defined pore radius and thus nucleation size is not strictly limited by pore size. The sparse strand structure will influence the nucleation process more weakly than in Vycor. The estimated  $R_c$  is larger than the mean strand distance, which means that the nucleated crystals were penetrated by tens of strands. It is probable that nucleation in aerogel is between the nucleation in bulk and the nucleation in pores: Nucleation size can have the temperature dependence reflecting the thermal and quantum nucleation as in bulk but heterogeneous nucleation at a small overpressure of a few mbars can be avoided due to nonwetting of crystals on the silica surface.

The measured pressure is that of the bulk crystals around the aerogel, and these crystals support the pressure gradient; there must be an error in the absolute value of the pressure on the order of 100 mbars [31]. Therefore, the obtained values of  $R_c$  should not be taken as an accurate value but should be regarded as a rough estimation of the order of magnitude. On the other hand, the pressure difference is likely to be obtained more accurately even in the presence of the pressure gradient and the fact that  $\delta P_{1/2}$  has a temperature dependence should be more robust.

In summary, nucleation probability of  $^4\text{He}$  crystals was measured in 98% porosity aerogel to investigate the nucleation process in disordered media. While temperature independent critical overpressure is expected in the PSL-nucleation model in which nucleation occurs when the critical nucleation size of the crystal matches the pore size, the measured mean critical overpressure has a characteristic temperature dependence in the aerogel. This dependence indicates that the crystal nucleates via macroscopic quantum tunneling in the low temperature avalanche region and via thermal activation in

the high temperature creep region. This supports the same conclusion drawn from the independent measurement of the crystallization rate. The nucleation process in highly porous materials is different from that in low porosity materials and has a hybrid character of the nucleation in bulk and in pores.

We would like to thank J. Pollanen and W. P. Halperin for providing us with aerogel samples supported by NSF Grant No.

DMR-0703656. This study was supported in part by the GCOE at Tokyo Institute of Technology “Nanoscience and Quantum Physics Project”, a Grant-in-Aid for Scientific Research (B) (Grant No. 21340095) and on Priority Areas (Grant No. 17071004) from the Ministry of Education, Culture, Sports, Science and Technology of Japan, and by a “Ground-based Research Announcement for Space Utilization” promoted by JAXA.

- 
- [1] J. G. Dash, A. W. Rempel, and J. S. Wettlaufer, *Rev. Mod. Phys.* **78**, 695 (2006).
- [2] S. Balibar, H. Alles, and A. Ya. Parshin, *Rev. Mod. Phys.* **77**, 317 (2005).
- [3] Y. Okuda and R. Nomura, *J. Phys. Soc. Jpn.* **77**, 111009 (2008).
- [4] J. P. Ruutu, P. J. Hakonen, J. S. Penttila, A. V. Babkin, J. P. Saramaki, and E. B. Sonin, *Phys. Rev. Lett.* **77**, 2514 (1996).
- [5] V. L. Tsymbalenko, *J. Low Temp. Phys.* **88**, 55 (1992).
- [6] V. L. Tsymbalenko, *J. Low Temp. Phys.* **121**, 53 (2000).
- [7] Y. Sasaki and T. Mizusaki, *J. Low Temp. Phys.* **110**, 491 (1998).
- [8] X. Chavanne, S. Balibar, and F. Caupin, *Phys. Rev. Lett.* **86**, 5506 (2001).
- [9] S. Balibar, T. Mizusaki, and Y. Sasaki, *J. Low Temp. Phys.* **120**, 293 (2000).
- [10] R. Nomura, Y. Suzuki, S. Kimura, and Y. Okuda, *Phys. Rev. Lett.* **90**, 075301 (2003).
- [11] H. Abe, F. Ogasawara, Y. Saitoh, T. Tatara, S. Kimura, R. Nomura, and Y. Okuda, *Phys. Rev. B* **71**, 214506 (2005).
- [12] R. Ishiguro, F. Caupin, and S. Balibar, *Europhys. Lett.* **75**, 91 (2006).
- [13] E. Tanaka, K. Hatakeyama, S. Noma, S. N. Burmistrov, and T. Satoh, *J. Low Temp. Phys.* **127**, 81 (2002).
- [14] F. Caupin and S. Balibar, *Phys. Rev. B* **64**, 064507 (2001).
- [15] H. Abe, M. Morikawa, T. Ueda, R. Nomura, Y. Okuda, and S. N. Burmistrov, *J. Fluid Mech.* **619**, 261 (2009).
- [16] E. D. Adams, K. Uhlig, Y.-H. Tang, and G. E. Haas, *Phys. Rev. Lett.* **52**, 2249 (1984).
- [17] E. D. Adams, Y. H. Tang, K. Uhlig, and G. E. Haas, *J. Low Temp. Phys.* **66**, 85 (1987).
- [18] J. R. Beamish, A. Hikata, L. Tell, and C. Elbaum, *Phys. Rev. Lett.* **50**, 425 (1983).
- [19] K. Yamamoto, Y. Shibayama, and K. Shirahama, *J. Phys. Soc. Jpn.* **77**, 013601 (2008).
- [20] K. Matsumoto, H. Tsuboya, K. Yoshino, S. Abe, H. Tsujii, and H. Suzuki, *J. Phys. Soc. Jpn.* **78**, 034601 (2009).
- [21] R. Nomura, A. Osawa, T. Mimori, K. I. Ueno, H. Kato, and Y. Okuda, *Phys. Rev. Lett.* **101**, 175703 (2008).
- [22] R. Nomura, H. Matsuda, R. Masumoto, K. Ueno, and Y. Okuda, *J. Phys. Soc. Jpn.* **80**, 123601 (2011).
- [23] F. Detcheverry, E. Kierlik, M. L. Rosinberg, and G. Tarjus, *Phys. Rev. E* **68**, 061504 (2003).
- [24] W. P. Halperin, H. Choi, J. P. Davis, and J. Pollanen, *J. Phys. Soc. Jpn.* **77**, 111002 (2008).
- [25] T. Herman, J. Day, and J. Beamish, *Phys. Rev. B* **73**, 094127 (2006).
- [26] H. Kato, W. Miyashita, R. Nomura, and Y. Okuda, *J. Low Temp. Phys.* **148**, 621 (2007).
- [27] H. Matsuda, R. Masumoto, A. Ochi, R. Nomura, and Y. Okuda, *J. Phys.: Conf. Ser.* **400**, 012044 (2012).
- [28] I. M. Lifshitz and Y. Kagan, *Zh. Eksp. Teor. Fiz.* **62**, 385 (1972) [*Sov. Phys. JETP* **35**, 206 (1972)].
- [29] M. Uwaha, *J. Low Temp. Phys.* **52**, 15 (1983).
- [30] E. Herbert, S. Balibar, and F. Caupin, *Phys. Rev. E* **74**, 041603 (2006).
- [31] M. W. Ray and R. B. Hallock, *Phys. Rev. B* **79**, 224302 (2009).